MATERIALS AND INTERFACES

# Development of a Novel Chemical-Looping Combustion: Synthesis of a Solid Looping Material of $NiO/NiAl_2O_4$

**Hongguang Jin, Toshihiro Okamoto, and Masaru Ishida***

*Research Laboratory of Resources Utilization, Tokyo Institute of Technology, 4259 Nagatsuta, Midori-Ku, Yokohama, Japan 226-8503*

A new kind of solid looping material, $NiO/NiAl_2O_4$, was synthesized based on integration of NiO, as solid reactant, with a composite metal oxide of $NiAl_2O_4$, as a binder, for applying it to chemical-looping combustion. The chemical looping combustion including reduction (fuel with metal) and oxidation (air with the reduced metal oxide) could make a breakthrough in simultaneous contribution to both energy and environmental issues. The reactivity of the reduction and oxidation was investigated by TGA (thermogravimetrical analysis). The results obtained here indicated that the new looping material, $NiO/NiAl_2O_4$, might significantly improve reaction rate, conversion, and regenerability in cyclic reaction, compared with the other materials. In addition, the carbon deposition can be completely avoided by addition of water vapor at a ratio of $H_2O/CH_4 = 2.0$. These results suggest that this new looping material of $NiO/NiAl_2O_4$ may play a vital role in developing chemical-looping combustion.

## 1. Introduction

It appears that we face a potentially serious problem of rapid climate change due to anthropogenic emissions of greenhouse gases (e.g. $CO_2$, $CH_4$, and $N_2O$). One of the options to overcome this problem is the development of $CO_2$ separation technologies from flue gases. However, most processes for $CO_2$ capture will consume a great amount of energy (i.e., a big energy penalty), which may reduce the plant's conversion efficiency, thereby resulting in a higher energy consumption with higher cost and additional production of $CO_2$. There is a major need to produce breakthrough ideas for new principles of fuel conversion, particularly in the area of combustion that would allow $CO_2$ capture in the flue gases or during combustion. For examples, some topics have paid attention to development of the new combustion such as $O_2/CO_2$−blown combustion, $H_2/O_2$ combustion, and partial oxidation in chemical gas turbine and combustion with high-temperature preheating of input air.

For the same purpose, we have proposed a novel gas turbine cycle with chemical-looping combustion and saturation for air.[1] The chemical-looping combustion may be carried out in two successive reactions between two reactors: fuel is oxidized by a metallic oxide in a reactor and then the resulting metal is oxidized by air in another reactor. The solid reactant as a looping material is cycled between the reduction and oxidation reactors. This combustion is completely different from the traditional one, and may provide the following advantages. (i) $CO_2$ capture takes place during combustion without energy penalty and with no need of special $CO_2$ separation equipment, since the composition of the exhaust gas from the reduction reactor is very simple, only in the presence of $CO_2$ and water vapor. The $CO_2$ is highly concentrated during reaction and may be easily recovered by condensation of water vapor. (ii) By using this process, $NO_x$ formation can be eliminated, without the use of deNOx technologies, since the fuel and air react in different reactors without in the absence of air and with no flame.[2] (iii) Breakthrough efficiency, an about 10−15% points higher thermal efficiency, can be achieved compared to the advanced combined cycle or IGCC power plant with $CO_2$ capture.[3] Therefore, this novel power plant may provide the dual contribution to simultaneous resolution of energy and environmental problems which cannot be achieved by any other current technologies.

Up to now, we have examined the NiO/YSZ, CoO/YSZ, and $Fe_2O_3$/YSZ (yttria stabilized zirconia) particles as looping reaction materials and experimentally investigated their reaction kinetics and carbon deposition behavior etc. by means of various particle preparation methods.[4] While some of the materials have good reactivity, their regenerability and resistance against carbon deposition are insufficient. It is therefore necessary to develop better looping materials.

In the present study, we have focused on various kinds of binders, instead of YSZ, and identified the fact that the interaction between solid reactants and binders is of extreme importance. Furthermore, we have synthesized a new looping material based on the addition of a new binder, $NiAl_2O_4$. It has suitable reactivity and regenerability under the conditions of the elevated pressures and avoidance of carbon deposition.

## 2. Experimental Section Apparatus

**2.1. Preparation of Solid Looping Materials.** We prepared nine kinds of looping materials based on the

* Corresponding author. Telephone: 81-45-9245254. Fax: 81-45-9245253. E-mail: ishida@res.titech.ac.jp.

10.1021/ie9803265 CCC: $18.00 
Published on Web 12/04/1998

**Table 1. Physical Property of Solid Particles**

| specimen | void fraction (%) | strength ($N/m^2$) |
|---|---|---|
| NiO/YSZ | 35.2 | $1.70 \times 10^7$ |
| $NiO/Al_2O_3$ | 22.4 | $2.98 \times 10^7$ |
| $NiO/NiAl_2O_4$ | 34.5 | $3.47 \times 10^7$ |

**Table 2. Solid Composition of Each Particle**

| | crystalline phase[a] | |
|---|---|---|
| specimen | fresh | after reduction |
| $NiO/Al_2O_3$ | NiO, $NiAl_2O_4$ | Ni, $NiAl_2O_4$, C |
| $NiO/TiO_2$ | NiO, $NiTiO_3$ | Ni, $NiTiO_3$, $TiO_2$, C |
| NiO/MgO | $Mg_{0.4}Ni_{0.6}O$ | $Mg_{0.4}Ni_{0.6}O$ |
| $CoO/Al_2O_3$ | $Co_3O_4$, $CoAl_2O_4$ | Co, $CoAl_2O_4$, C |
| $CoO/TiO_2$ | $Co_3O_4$, $CoTiO_3$ | Co, $CoTiO_3$, $TiO_2$, C |
| CoO/MgO | $Mg_{0.4}Co_{0.6}O$ | $Mg_{0.4}Co_{0.6}O$ |
| $Fe_2O_3/Al_2O_3$ | $Fe_2O_3$, $Al_2O_3$ | $Fe_2O_3$, $Al_2O_3$, $Fe_3C$ |
| $Fe_2O_3/TiO_2$ | $Fe_2TiO_5$, $TiO_2$ | $Fe_2TiO_5$, $TiO_2$, $Fe_3C$ |
| $Fe_2O_3$/MgO | $MgFe_2O_4$, MgO | $MgFe_2O_4$, MgO |

[a] Obtained from XRD pattern and EDX.

three kinds of solid looping reactants and three kinds of additive materials. The solid looping reactants of metal oxides, NiO, CoO, and $Fe_2O_3$, are chosen based on their ability to resist melting and vaporization at high temperature. The additive materials selected here are $Al_2O_3$, $TiO_2$, and MgO, which act as binders. The $Al_2O_3$ and MgO binder-based particles were made by the dissolution method as follows.[4]

For example, aluminum nitrate enneahydrate and nickel(II) (cobalt or iron) nitrate hexahydrate were dissolved into mixture of 2-propanol and water so that the weight ratios of metal oxides to additive materials would become 6:4. This solution was stirred for 1 h and was dried at 373 K for 12 h, at 423 K for 24 h, and at 473 K for 5 h and then was calcined at 773 K for 3 h in an air atmosphere. By this method, 2-propanol, water, and nitric acid in the solution can be evaporated off at different stages, thereby offering production of fine and porous powder.[5,6] Spherical particles were made from the paste obtained by adding water to the resultant powder. These particles were dried at 353 K for 30 min and calcined in air at 1573 K for 6 h. The $TiO_2$-based particles were made from the mixture of the metal oxide powders.[7] The mixed powder was ground for 2 h by pestle and mortar. The procedures of particle shaping, drying, and calcination were similar to those by the above dissolution method. The physical property and composition of solid particles are listed in Tables 1 and 2.

**2.2. Experimental Apparatus.** Figure 1 is a schematic diagram of thermogravimetrical analyzer apparatus (Mac Science, TG-DTA 2000S) that can handle a weight as small as 10 $\mu$g. The specimen particle was placed on a 3 mm diameter $Al_2O_3$ pan situated on the sample arm of the balance. Gaseous reactants, for which flow rates were regulated by mass flow controllers in the gas-supplier unit, were fed into reaction unit, and in some runs this stream was saturated with distilled water at specified temperatures. The total flow rate was of 100 mL/min (STP) and the stream from gas-supplier unit was heated to keep water vapor from condensing. Inert gas (Ar) was fed into the weighing unit to prevent the reactant gas from diffusing into the microbalance chamber. When the temperature reached the specified value by use of an electric furnace, two four-port switching valves changed the gaseous stream from Ar to reactant. The weights of the reactant

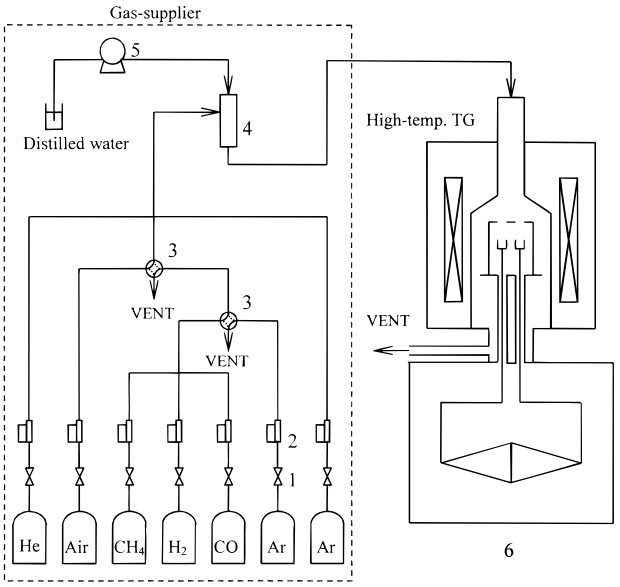


1. Regulator, 2. Mass flow controller, 3. 4-port switch valve, 4. Evaporator, 5. Micro-pump, 6. Micro-balance

**Figure 1.** Schematic diagram of TG reactor.

specimens and the reaction temperatures were continuously recorded by a computer.

For solid particles, structural properties such as crush strength, average pore size, and XRD chemical phase were measured. The microstructures of particles were identified by SEM (scanning electron microscope, JEOL JSM-6300). The distribution of solid components in particles was analyzed by EDX (energy-dispersive X-ray microanalyzer, JEOL JED-2100). Also, the crystal structures of solid looping materials were identified by XRD from diffraction patterns between $2\theta = 10°$ and 70° obtained with an X-ray diffractometer.

## 3. Results and Discussion

**3.1. An Outstanding Property of Regenerability.** Regenerability is one of the fatal problems for application of chemical-looping combustion. For example, the NiO/YSZ particle made from the dissolution method has good reactivity but was broken with cracks on the surface layer of the particle, after five cycles.

Figure 2 depicts the excellent regenerability of a solid looping particle of NiO with addition of $NiAl_2O_4$, where the spherical particle of 2.1 mm diameter was reduced by $H_2$ at 873 K and the reduced particle was oxidized by air at 1273 K. As shown in the figure, fractional oxidation is defined by $X = 1 - (W_{oxd} - W)/(W_{oxd} - W_{red})$, where $W$ is instantaneous weight and $W_{oxd}$ and $W_{red}$, respectively, are the completely oxidized weight (initial weight) and the completely reduced weight. Unity on the ordinate corresponds to NiO and zero to Ni. For the early few cycles, rates of reduction and oxidation were slightly changed, but they were almost the same after the ninth cycle. In particular, the particles after the cyclic reactions were not broken and looked like the fresh ones. This excellent performance has not been shown by the other materials examined here.

Then, the regenerability of this looping material was examined for the use of humidified $CH_4$ as fuel. The reduction and oxidation temperatures were 973 and 1273 K, and the $H_2O/CH_4$ ratio was 2.0. As the left side

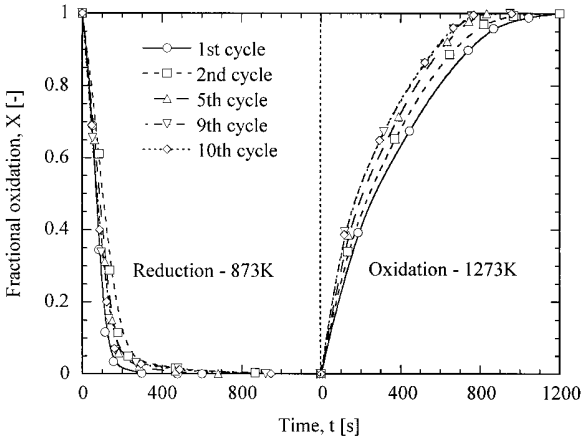


**Figure 2.** Regenerability of $NiO/NiAl_2O_4$ with $H_2$ and air.

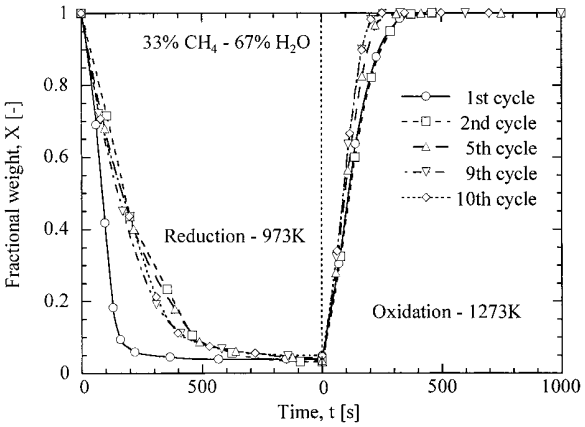


**Figure 3.** Repeatability of $NiO/NiAl_2O_4$ by $CH_4$-fueled gas.

of Figure 3 represents, the reduction rate was apparently decreased in the second cycle, but after that, a drastic change in reactivity was not observed. The oxidation rate slightly increased as the cyclic reaction proceeded. After the ninth cycle, however, no difference was observed.

Figure 4 shows the cross-sectional photos obtained from SEM, in which the fresh particles have round grains of 0.5−2.0 $\mu$m diameter and also small pores. It is worth noticing that the microstructures of the fresh particle and the particles after the first cycle and after the 10th cycle were not drastically changed, compared to the other materials. Namely, the microstructure of the $NiO/NiAl_2O_4$ was relatively stable in the course of the cyclic reaction. In addition, as Table 1 shows, the crush strength of the $NiO/NiAl_2O_4$ particle is $3.5 \times 10^7$ N/m$^2$, about two times higher than that of NiO/YSZ ($1.7 \times 10^7$ N/m$^2$).

Accordingly, this new looping material has not only good reactivity but also an outstanding regenerability. By overcoming this crucial obstacle, we have made progress in realizing a chemical looping combustion.

**3.2. Synthesis of a Looping Material by Addition of a New Binder of $NiAl_2O_4$.** The new looping material in the previous section was synthesized and based on experimentally examining various combinations of binders of $Al_2O_3$, $TiO_2$, and MgO and solid reactants of metal oxides of NiO, CoO, and $Fe_2O_3$. It is noted that in the course of calcination of these particles, complex compounds had been formed between solid reactants and additive materials, except in the case

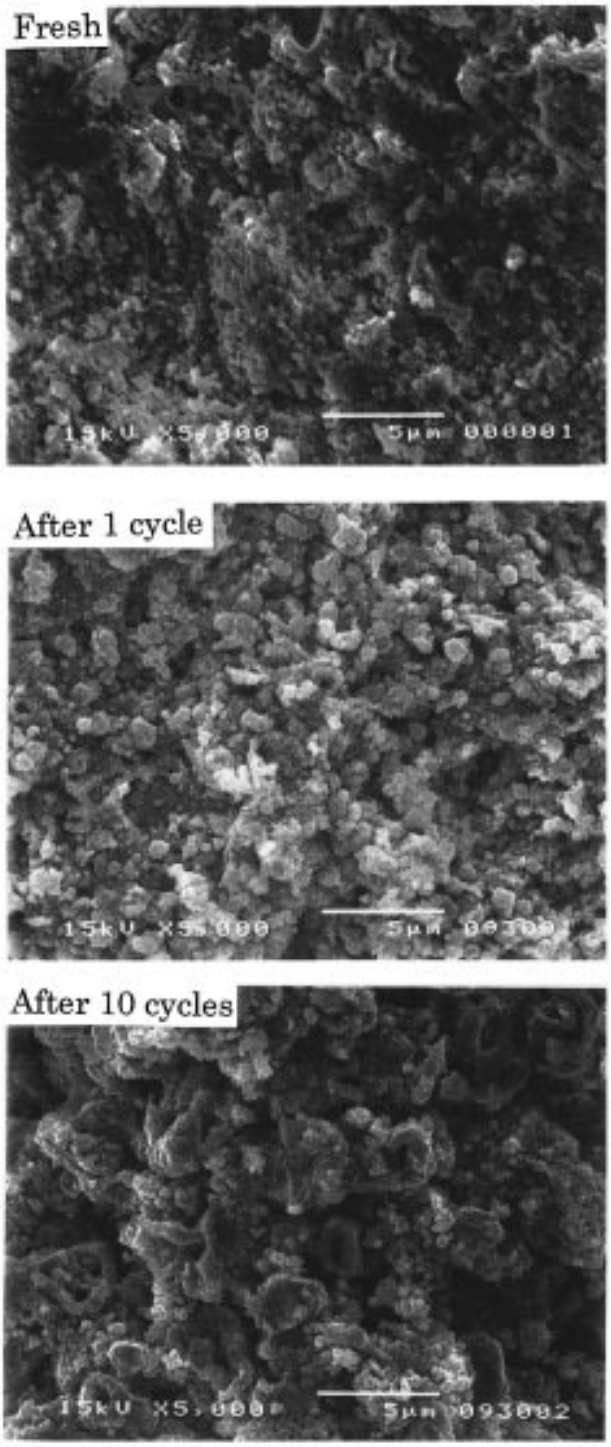


**Figure 4.** SEM of cross-sectional photos of $NiO/NiAl_2O_4$ in the cyclic reaction.

between $Fe_2O_3$ and $Al_2O_3$. Table 2 shows the solid composition of the fresh material and the reduced particle, determined from XRD.

Figure 5 presents the reactivity of reduction and oxidation for the nine kinds of particles. The weight ratios of solid reactants to binders were set at 6:4. Spherical particles of 1.8 mm diameter were used. The reduction and oxidation temperatures, respectively, were 873 and 1273 K. The left- and right-hand sides of this figure correspond to the reduction of metal oxide by $H_2$ and the oxidation of the reduced metal by air,

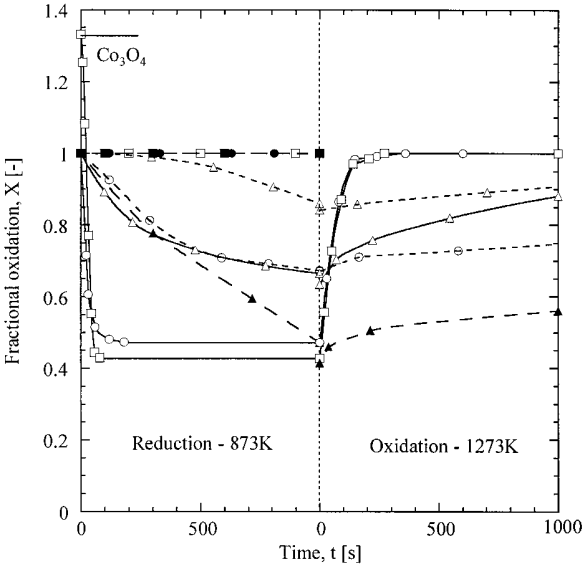


**Figure 5.** Effect of solid reactant and binder on reactivity. Key: (−○−) $NiO/Al_2O_3$; (−□−) $CoO/Al_2O_3$; (−△−) $Fe_2O_3/Al_2O_3$; (--○--) $NiO/TiO_2$; (--□--) $CoO/TiO_2$; (--△--) $Fe_2O_3/TiO_2$; (−●−) NiO/MgO; (−■−) CoO/MgO; (−▲−) $Fe_2O_3$/MgO.

respectively. For cobalt, $Co_3O_4$ is a stable oxide at low temperature, but CoO becomes stable at above 1273 K. Hence, CoO gives $X = 1$.

First, for materials with addition of $Al_2O_3$, the reduction of $NiO/Al_2O_3$ and $CoO/Al_2O_3$ particles were very fast, but reduction conversions were not high, only $X =$ 0.46 and 0.42, respectively. Since compounds of the spinel type of $NiAl_2O_4$ and $CoAl_2O_4$ are formed and they are stable, the free amount of metal oxide reactant is decreased, and hence it gives rise to a lower reduction conversion. After reduction of each material, the oxidations of $Ni/NiAl_2O_4$ and $Co/CoAl_2O_4$ particles were also very fast and the final weights of oxidation returned to the initial ones. In contrast to these cases, for the particle of $Fe_2O_3/Al_2O_3$, such a complex compound was not formed, and both reduction and oxidation were very slow.

Second, for particles with $TiO_2$, they had very slow reduction and oxidation as well as low conversion. Complex compounds were also formed, but they are unstable in reduction, and hence the solid reactant can be reduced to metal by $H_2$. The very low reduction rate is caused by a small amount of pores or platelike grains, as shown in Figure 6.

Finally, for particles with MgO, no reduction took place except for $Fe_2O_3$/MgO, since all reactants of NiO and CoO were consumed to form the stable solid solution of $Mg_{0.4}Ni_{0.6}O$ and $Mg_{0.4}Co_{0.6}O$. In addition, $Fe_2O_3$/MgO had slow reduction (from $X = 1$ to $X = 0.4$ in 3000 s) and oxidation (from $X = 0.4$ to $X = 0.55$ in 1000 s).

Of the above materials, we have paid attention to $Al_2O_3$-based materials due to their higher reaction rates. An important point is that when $Al_2O_3$ is used as additive in NiO particles, although a compound of the spinel type of $NiAl_2O_4$ is formed, it is stable below a temperature of 1173 K. Hence, by making use of this feature, we have synthesized a looping material of $NiO/NiAl_2O_4$ by addition of a new binder of $NiAl_2O_4$, instead of $Al_2O_3$ (i.e., $NiO:NiAl_2O_4 = 6:4$).

In Figure 7 the reactivity of this new material is compared with that of the other two materials. It is clear that both reduction and oxidation rates of this new

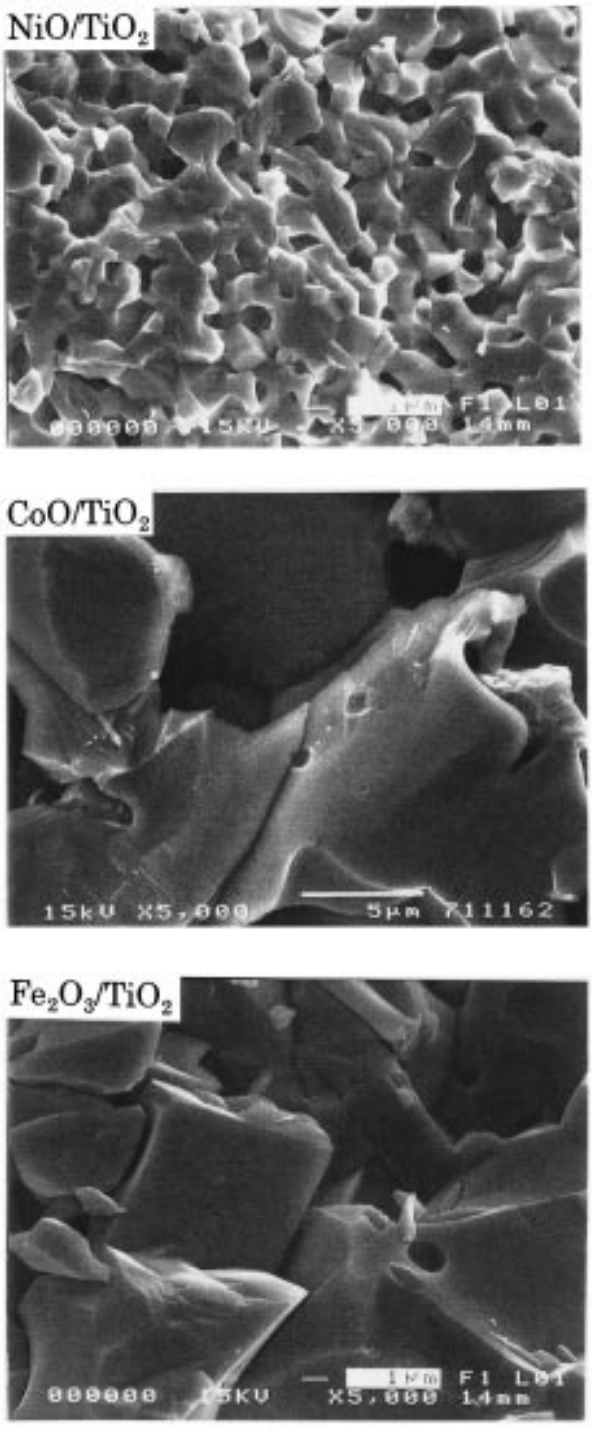


**Figure 6.** SEM of cross-sectional photos of $TiO_2$ added particles.

material are very high compared to those of previous materials. In particular, both reactions can be completely performed, compared to the previous material ($NiO/Al_2O_3$). Another advantage is that the material cost of $NiAl_2O_4$ is much lower than that of YSZ, nearly 20% of YSZ. For this reason, we have examined this new material in more detail, such as the reactivity on the elevated pressure and the ability to avoid carbon deposition.

**3.3. The Effect of Pressure on Reactivity.** The effect of pressure on reactivity was examined by use of high-pressure TGA. The pressures were elevated to the specified values (3 and 9 atm), and then the tempera-

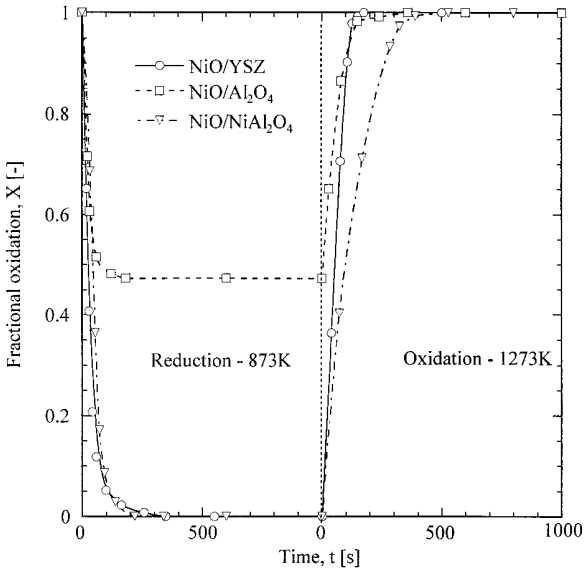


**Figure 7.** Effect of binder on reactivity.

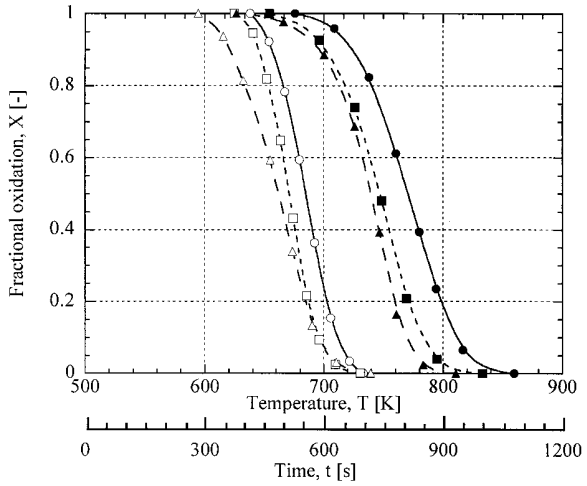


**Figure 8.** Effect of material on reduction under the elevated pressure. Key: (−○−) NiO/YSZ, 1 atm; (−●−) NiO/$NiAl_2O_4$, 1 atm; (--□--) NiO/YSZ, 3 atm; (--■--) NiO/$NiAl_2O_4$, 3 atm; (−△−) NiO/YSZ, 9 atm; (−▲−) NiO/$NiAl_2O_4$, 9 atm.

tures were increased at a rate of 20 K/min. Hence, the reaction times correspond to the temperatures shown in Figures 8 and 9.

The diameter of NiO/$NiAl_2O_4$ particle was 1.8 mm. For reduction, the initial rates of the pressurized reduction were low compared to that in Figure 7 due to their lower temperatures at the beginning of the reaction. With an increase in pressure the reduction took place at lower temperatures (decreased by about 50 K) as shown in Figure 8 (black marks), and the material was completely reacted prior to reaching a temperature of 873 K.

For oxidation, as the pressure was increased, the starting temperature of oxidation was lowed and its oxidation rate was nearly independent of pressure, as shown in Figure 9. In comparison of NiO/YSZ particle, the reduction temperatures of the NiO/$NiAl_2O_4$ particle were increased by 50 K, as shown in Figure 8, and the oxidation temperatures were decreased by 100 K in Figure 9.

**3.4. Avoidance of Carbon Deposition.** Figure 10 illustrates carbon deposition behavior for particles of

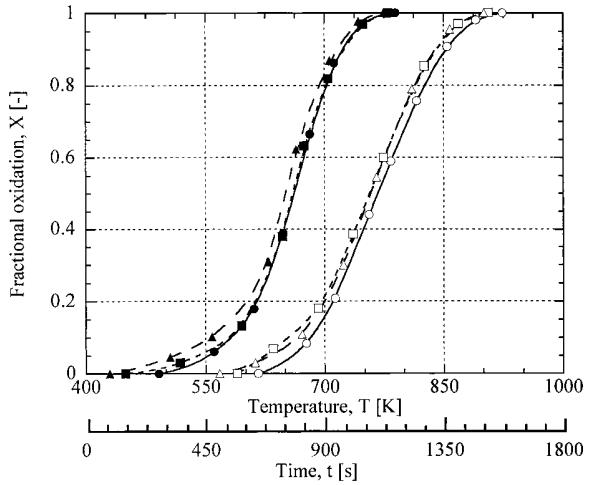


**Figure 9.** Effect of material on oxidation under the elevated pressure. Key: (−○−) NiO/YSZ, 1 atm; (−●−) NiO/$NiAl_2O_4$, 1 atm; (--□--) NiO/YSZ, 3 atm; (--■--) NiO/$NiAl_2O_4$, 3 atm; (−△−) NiO/YSZ, 9 atm; (−▲−) NiO/$NiAl_2O_4$, 9 atm.

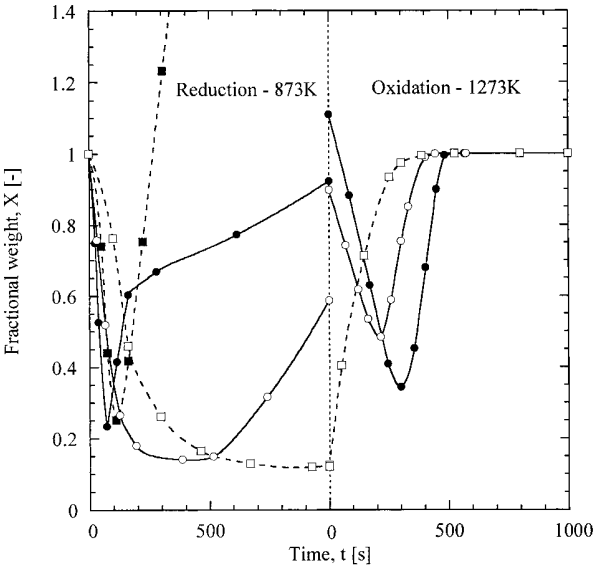


**Figure 10.** Effect of a double oxide particle on carbon deposition. Key: (−●−) NiO/YSZ ($CH_4$); (−○−) NiO/YSZ ($H_2O/CH_4$ = 2.0); (--■--) NiO/$NiAl_2O_4$ ($CH_4$); (--□--) NiO/$NiAl_2O_4$ ($H_2O/CH_4$ = 2.0).

NiO/YSZ and NiO/$NiAl_2O_4$. A particle of 50 mg was set on the sample arm of the balance in TG. Left- and right-hand sides of this figure correspond to the reduction of metal oxide by pure $CH_4$ and the saturated $CH_4$ at 873 K and the oxidation of the reduced metal by air at 1273 K.

On the left-hand side of Figure 10, the weights of the specimens were initially decreased by reduction of metal oxide according to reaction 1, in which M referred to metal, and MO to metal oxide.

$$CH_4 + 4MO \rightarrow CO_2 + 2H_2O + 4M \qquad (1)$$

After that, the weights of particles were sharply increased due to carbon deposition.

$$CH_4 \rightarrow C + 2H_2 \qquad (2)$$

$$CO \rightarrow {}^1/_2C + {}^1/_2CO_2 \qquad (3)$$

The former (i.e., decomposition of $CH_4$) reaction is the endothermic reaction, and the latter (i.e., decomposition of CO) is the exothermic reaction. In the previous study,[8] we have discussed a carbon deposition caused by reaction 3 in coal gas. Here, the carbon deposition is mainly caused by decomposition of $CH_4$ (reaction 2).

As a result, $NiO/NiAl_2O_4$ particle was swollen by the deposited carbon and was broken into small fragments. The distribution of C, Ni, and Al in the particle of $NiO/NiAl_2O_4$, after reduction by pure $CH_4$ at 873 K for 200 s, was analyzed by EDX and BEI (backscattered ion image). The result indicated that the distribution of C was relatively analogous to that of Ni and was just the opposite of that of Al (i.e., $NiAl_2O_4$).

This fact suggested that the reduced Ni in NiO, instead of $NiAl_2O_4$, might cause carbon deposition and that NiO in the aluminate ($NiAl_2O_4$) was stable enough[9] not to promote carbon deposition.[10−12] The crystalline phases of the specimens at the fresh state and the reduced state by $CH_4$ were shown in Table 2. It is to be noted that the deposited carbon on the $NiO/NiAl_2O_4$ particle was elemental carbon and no nickel carbides were formed. In addition, from the void fraction of each specimen listed in Table 1, we may find that the $NiO/NiAl_2O_4$ particle has a higher void fraction than other mediums. Thus, the Ni having a high void fraction may act as a catalyst and cause a higher rate of carbon deposition.

Next, to avoid the carbon deposition, $CH_4$ was saturated at a ratio of $H_2O/CH_4 = 2.0$. The carbon deposition behavior during reduction by the saturated $CH_4$ was also shown in the left-hand side of Figure 10 (open symbols). It is found that $NiO/NiAl_2O_4$ had no weight increase after saturation of fuel, i.e., no carbon deposition. The addition of water vapor may cause the steam reforming (4) and shift reaction (5).

$$CH_4 + H_2O \rightarrow CO + 3H_2 \quad (4)$$

$$CO + H_2O \rightarrow CO_2 + H_2 \quad (5)$$

The products of $H_2$ and CO from the above reactions might also proceed to give further reduction of metal oxide, (6) and (7).

$$H_2 + MO \rightarrow H_2O + M \quad (6)$$

$$CO + MO \rightarrow CO_2 + M \quad (7)$$

By addition of water vapor at the ratio of $H_2O/CH_4 = 2.0$, carbon deposition could be completely avoided in $NiO/NiAl_2O_4$ particle, but not in the NiO/YSZ particle. In other words, this new material is strongly dependent on the addition of water vapor for complete avoidance of carbon deposition.

Oxidation of the above solid particles, after reduction by $CH_4$, was shown on the right-hand side of Figure 10. The weights of NiO/YSZ particles with and without water vapor were initially decreased due to oxidation of the deposited carbon and then returned to the initial weights. Comparatively, the weight of $NiO/NiAl_2O_4$ was monotonically increased to unity. It indicated that the expected oxidation is obtained.

In general, we can find from the above examination that this new looping material, $NiO/NiAl_2O_4$, is a suitable material for application in chemical looping combustion, since it has an excellent overall performance in areas such as reactivity, outstanding regenerability, and complete avoidance of carbon deposition.

## Conclusions

To find a suitable looping material for chemical looping combustion that may make a breakthrough in simultaneous contribution to efficient use of energy and mitigation of greenhouse gas, we have performed experimental investigations by combining a solid reactant, NiO, CoO, or $Fe_2O_3$, with a binding material, $Al_2O_3$, $TiO_2$, or MgO. Also, we have developed a new looping material of $NiO/NiAl_2O_4$ by the integration of NiO with the spinel-type metal oxide of $NiAl_2O_4$. This new material is able to give complete conversion and fast rates for looping reactions (reduction and oxidation). In particular, this material has excellent regenerability in cyclic use, which is one of key factors for application of this combustion. The carbon deposition can be completely avoided at a ratio of $H_2O/CH_4 = 2.0$. These promising results suggest that this new looping material of $NiO/NiAl_2O_4$ will provide an outstanding performance for a solid looping material in chemical-looping combustion.

## Acknowledgment

This research was supported by New Energy and Industrial Technology Development Organization (NEDO), as a project of the “Proposal-Based Advanced Industrial Technology R & D Program”, and by the Research Institute of Innovative Technology for the Earth (RITE) in Japan.

## Literature Cited

(1) Ishida, M.; Jin, H. A New Advanced Power-Generation System Using Chemical-looping Combustion. *Energy—Int. J.* **1994**, *19*, 415.

(2) Ishida, M.; Jin, H. A Novel Chemical-looping Combustor without NOx Formation. *Ind. Eng. Chem. Res.* **1996**, *35*, 2469.

(3) Jin, H.; Ishida, M. A New Advanced IGCC Power Plant with Chemical-looping Combustion. *Proceedings of Thermodynamic Analysis and Improvement of Energy System*; Beijing World Publishing Corp.: Beijing, 1997; p 548.

(4) Ishida, M.; Jin, H.; Okamoto, T. A Fundamental Study of a New Kind of Medium Material for Chemical-looping Combustion. *Energy Fuels* **1996**, *10*, 958.

(5) Takahashi, K.; Okubo, T.; Nagamoto, H. Production of Porous YSZ film based on the Sol−gel method. *Proceedings of the 26th Japan National Chemical Engineering Conference, (in Japanese)*; The Society of Chemical Engineers, Japan: Kyoto, 1993; p 165.

(6) Saka, S. *Science of Sol−Gel Processing*; Gurahe Publisher: Tokyo, 1988.

(7) Ishida, M.; Jin, H. A Novel Combustor Based on Chemical-looping Reaction and its Reaction Kinetics. *Chem. Eng. Jpn.* **1994**, *27*, 296.

(8) Ishida, M.; Jin, H.; Okamoto, T. Kinetic Behavior of Solid Particle in Chemical-looping Combustion: Suppressing Carbon Deposition in Reduction. *Energy Fuels* **1998**, *12*, 223.

(9) Numaguchi, T.; Kikuchi, K. Deactivation of Bimodal Nickel Catalyst for Steam Methane Reforming Reaction. *Ind. Eng. Chem. Res.* **1991**, *30*, 447.

(10) Claridge, J. B.; Green, M. L. H.; Trang, S. C.; York, A. P. E.; Ashcroft, A. T.; Battle, P. D. A Study of Carbon Deposition on Catalysts during the Partial Oxidation of Methane to Synthesis Gas. *Catal. Lett.* **1993**, *22*, 299.

(11) Numaguchi, T.; Shoji, K.; Yoshida, S. Hydrogen Effect on $\alpha$-$Al_2O_3$ Supported Ni Catalyst for Steam Methane Reforming Reaction. *Appl. Catal.* **1995**, *133*, 241.

(12) Sacco, A.; Geurts, F. W. A. H.; Jablonski, G. A.; Lee, S.; Gately, R. A. Carbon Deposition and Filament Growth on Fe, Co, and Ni Foils Using $CH_4-H_2-H_2O-CO-CO_2$ Gas Mixtures. *J. Catal.* **1989**, *119*, 322.

*Received for review* May 26, 1998
*Revised manuscript received* October 2, 1998
*Accepted* October 16, 1998

IE9803265